International Journal of Mechanical, Industrial and Aerospace Sciences
ISSN: 2517-9950
Vol:8, No:5, 2014

A Numerical Model Simulation for an Updraft Gasifier Using High Temperature Steam

T. M. Ismail, M. Abd El-Salam

***Abstract*—**A mathematical model study was carried out to investigate gasification of biomass fuels using high temperature air and steam as a gasifying agent using high-temperature air up to 1000°C. In this study, a 2D computational fluid dynamics model was developed to study the gasification process in an updraft gasifier, considering drying, pyrolysis, combustion, and gasification reactions. The gas and solid phases were resolved using a Euler−Euler multiphase approach, with exchange terms for the momentum, mass, and energy. The standard k−ε turbulence model was used in the gas phase, and the particle phase was modeled using the kinetic theory of granular flow. The results show that the present model giving a promise way in its capability and sensitivity for the parameter affects that influence the gasification process.

***Keywords*—**Computational fluid dynamics, gasification, biomass fuel, fixed bed gasifier.

I. Introduction

THE conversion of biomass materials has the precise objective to transform a carbonaceous solid material, which is originally difficult to handle, bulky and low energy concentration, into higher energy density fuels that permit easy storage and transfer through conventional pumping and transport systems [1]. Gasification is a chemical conversion process of any carbonaceous into a process or fuel gases with a useable heating value. The term 'fuel gases' represent gases that are destined for combustion purposes and their heat of combustion is of great importance, whereas 'process gases' are produced in chemical synthesis processes [2].

The gasification process requires some gasifying agent that provides oxygen for the formation of CO from solid carbon in the fuel. The gasifying agents include air, oxygen, steam, and CO2. The most common agent is air because of its extensive availability at no cost [3]. Steam is another alternative. The key advantage is that it increases the hydrogen content of the product gas. Furthermore, the production of tars is minimized, in particular at high steam temperatures. The presence of steam is important to further catalytic upgrading of the product syngas [4].

Numerical simulations have become popular in recognizing the complex gas–solid flow behaviors as in [5] and chemical reactions [6], which can offer the detailed information about the gasification processes and bridge the gap effectively between large-scale commercialized beds and small scale testing models. For gas–solid flow, two different calculation models can be used to describe the complex gas–solid flow behaviors. They are the trajectory model and the continuum description model [6]. As a most popular trajectory model, discrete element method (DEM) offers a more natural way to simulate gas–solid flow [7], but it becomes more and more computational expensive (CPU and memory resource requirements) as the number of particles increases. Eulerian approach is the other popular method for describing gas–solid flow due to little CPU and memory resource requirements [8]. In most recent continuum models constitutive equations according to the kinetic theory of granular flow (KTGF) are incorporated [9]. Benyahia et al. [10] and Zhong et al. [11] also applied KTGF to study the dense gas–solid flow characteristics of circulating fluidized bed and spout-fluid bed, respectively. Although numerical calculation has been widely used to simulate the gas–solid flow in fluidized beds, there has been little study on the simulation of gas–solid flow coupling with chemical reactions in updraft and downdraft gasifiers. Two methods could couple gas–solid flow with chemical reactions based on DEM and Eulerian approaches, respectively. For DEM-based simulation, the natural framework for the implementation of the physical models is offered. But it is computationally expensive, especially when the chemical reactions are added [12]. The other method, Eulerian-based simulation, has been used by Yu et al. [13] to simulate coal gasification in a bubbling fluidized bed gasifier.

The mathematical model of the gasifier in the present work will be simulated using a new development code, namely COMMENT-Code (Combustion Mathematics and Energy Transport) [14] to simulate the processes rate and combustion process within the bed. The model will be divided into two parts; firstly the process rate models and then the transport equation model for gas and solid phases. Validation of the code developed in the current study is conducted through experimental results for the HTAG process of biomass fuels [15].

II. Experimental Setup

Fig. 1 shows the HTAG test facility that has been built at KTH-Royal Institute of Technology. This system has been described in a previous publication [16], [17]. The height of the gasifier is 3200mm with an internal diameter of 400mm. The produced gas flows out of the reactor at the top.

T.M. Ismail is with the Department of Mechanical Engineering, Suez Canal University, Ismailia, Egypt (e-mail: tamer.ismail@eng.suez.edu.eg; temoil@aucegpt.edu).

M. Abd El-Salam is with the Department of Basic Science, Cairo. University, Giza, Egypt (e-mail: mohamedelsheikh@cu.edu.eg).

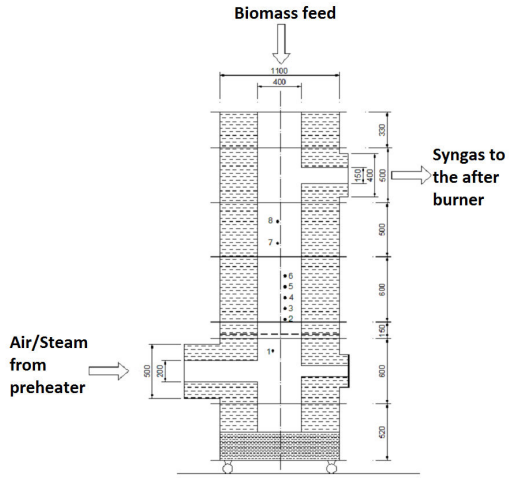

Fig. 1 Cross section of the gasifier

III. Computational Fluid Dynamics Simulation

The developed model presented in the current work to solve the governing equations of mass, momentum and energy, by means of a multi-fluid Eulerian model incorporating the Kinetic Theory of Granular Flow (KTGF), taking under consideration the process rates.

A. Process Rate Equations

1. Drying

The rate of moisture release from solids can be expressed as [18]:

$$\mathrm{R_{evp}} = \mathrm{A_s h_s}\left(\mathrm{C_{w,s}} - \mathrm{C_{w,g}}\right) \mathrm{T_s} < 100℃ \tag{1}$$

$$\text{or } \mathrm{R_{evp}} = \frac{\mathrm{Q_{cr}}}{\mathrm{H_{evp}}} \mathrm{T_s} = 100℃ \tag{2}$$

$$\mathrm{Q_{cr}} = \mathrm{A}\left(\mathrm{h_s'}\left(\mathrm{T_g} - \mathrm{T_s}\right) + \epsilon\delta(\mathrm{T_\infty^4} - \mathrm{T_s^4})\right) \tag{3}$$

2. Pyrolysis

The pyrolysis is very important in updraft gasifier, where the volatilization of the biomass is assumed to give rise to volatile species and char [19].

$$R_v = -\rho_{sb}\frac{dY_v}{dt} = \rho_{sb} Y_v A_v exp\left(\frac{E_v}{RT}\right)$$
$$A_v = 3.63 \times 10^4\ {}^1\!/_S\ , \frac{E_v}{R} = 9340\ K \tag{4}$$

3. Gasification

The gaseous fuels released from the pyrolysis process have first to mix with the surrounding gasification agent before their chemical reaction can occur. In this model, the actual reaction rates of volatile species are taken as [14]:

$$R = min[R_{kin}, R_{mix}] \tag{5}$$

$$R_{mix} = C_{mix}\rho_g \times A \times B \tag{6}$$

$$A = 150\frac{D_g(1-\phi)^{2/3}}{d_p^2\phi} + 1.75\frac{V_g(1-\phi)^{1/3}}{d_p\phi} \tag{6a}$$

$$B = min\left\{\frac{C_{fuel}}{S_{fuel}}, \frac{C_{O_2}}{S_{O_2}}\right\} \tag{6b}$$

The rate for each species is given by the following expressions;

$$R_{CH_4} = 59.8\, T_g P^{0.3} exp\left(\frac{-12{,}200}{T_g}\right) C_{CH_4}^{0.5} \tag{7}$$

$$R_{CO} = 1.3 \times 10^{11} exp\left(\frac{-62{,}700}{T_g}\right) C_{CO} C_{H_2O}^{0.5} C_{O_2}^{0.5} \tag{8}$$

$$R_{H_2} = 3.9 \times 10^{17} exp\left(\frac{-20{,}500}{T_g}\right) C_{H_2}^{0.85} C_{CH_4}^{0.56} C_{O_2}^{1.42} \tag{9}$$

$$R_{wg} = 2.78\ exp\left(\frac{-12600}{RT_g}\right)\left(C_{CO}C_{H2O} - \frac{C_{CO2}C_{H2}}{0.0265exp(65800/RT_g)}\right) \tag{10}$$

$$R_{sr} = 0.3 \times 10^9 exp\left(\frac{-125400}{RT_g}\right) T \times C_{CnH2n+2} C_{H2O} \tag{11}$$

4. Combustion

$$C + \alpha O_2 \rightarrow 2(1-\alpha)CO + (2\alpha - 1)CO_2$$
$$\alpha = \frac{CO}{CO_2} = 2500exp\left(\frac{-6420}{T}\right) \tag{12}$$

For temperatures between 730 and 1170 K

$$R_c = \frac{P_{O_2}}{\frac{1}{K_r} + \frac{1}{K_d}} \tag{13}$$

$$K_d = \frac{5.06 \times 10^{-7}}{d_p} \times \left(\frac{T_s + T_g}{2}\right)^{0.75} \tag{14}$$

$$K_r = A_c T_s exp\left[\frac{E_c}{RT_s}\right] \tag{15}$$

$\mathrm{A_c}$ = 3 kg/m² s kPa and $\mathrm{E_c}/\mathrm{R}$ = 10300 K

B. Transport Equations for Gas and Solid Phases

1. Continuity Equation

Gas Phase:

$$\frac{\partial(\phi\rho_g)}{\partial t} + \nabla\left(\phi\rho_g u_g\right) = S_{sg} \tag{16}$$

Solid Phase:

$$\frac{\partial\left((1-\phi)\rho_s\right)}{\partial t} + \nabla\left((1-\phi)\rho_s u_s\right) = -S_{sg} \tag{17}$$

$$S_{sg} = R_{evp} + R_v + R_c \tag{18}$$

2. Momentum Equation

Gas Phase:

$$\frac{\partial(\phi\rho_g u_g)}{\partial t} + \nabla\left(\phi\rho_g u_g u_g\right) = -\phi\nabla P_g + \phi\rho_g g - \beta\left(u_g - u_s\right) + \nabla\phi\tau_g \tag{19}$$

The gas–solid inter-phase drag coefficient, β, is calculated as follows [20], [21];

$$\beta = 150\frac{(1-\phi)^2\mu_T}{\phi d_p^2} + 1.75\frac{\rho_g(1-\phi)|U_g - U_s|}{d_p} \quad (20)$$

The gas phase stress tensor as follows;

$$\tau_g = \mu_g\left[\nabla u_g + \nabla u_g^T\right] - \frac{2}{3}\mu_T(\nabla u_g) \quad (21)$$

$$\mu_T = \mu_g + \mu_t \quad (22)$$

$$\mu_t = \rho_g C_\mu \frac{k^2}{\varepsilon} \quad (23)$$

$C_\mu$is the constant, which is set as 0.09.

The governing transport equations for k and ε respectively are:

$$\frac{\partial}{\partial t}(\phi\rho_g k) + \nabla(\phi\rho_g u_g k) = +\nabla\left(\phi\frac{\mu_t}{\sigma_k}\nabla k\right) + \phi G_k - \phi\rho_g\epsilon \quad (24)$$

$$\frac{\partial}{\partial t}(\phi\rho_g\varepsilon) + \nabla(\phi\rho_g u_g\varepsilon) + \nabla\left(\phi\frac{\mu_t}{\sigma_\varepsilon}\nabla\varepsilon\right) + \phi\left(C_{\varepsilon1}G_k - C_{\varepsilon2}\rho_g\epsilon\right) \quad (25)$$

In the above equations G_k represents the generation of turbulence kinetic energy due to the mean velocity gradients and is expressed as follows;

$$G_k = \mu_t\nabla u_g.\left[\nabla u_g + \nabla u_g^T\right] - \frac{2}{3}\nabla u_g\left(\mu_t\nabla u_g + \rho_g k\right) \quad (26)$$

$C_{\varepsilon1}$= 1.44 and $C_{\varepsilon2}$ = 1.92, the turbulent Prandtlnumbersfork and ε are σ_k = 1 and σ_ε = 1.3, respectively [22].

Solid Phase:

$$\frac{\partial((1-\phi)\rho_s u_s)}{\partial t} + \nabla((1-\phi)\rho_s u_s u_s) = -(1-\phi)\nabla P_s + (1-\phi)\rho_s g - \beta(u_g - u_s) + \nabla(1-\phi)\tau_s \quad (27)$$

where the stress tensor of the solid phase is expressed as follows;

$$\tau_s = \left(\mu_b - \frac{2}{3}\mu_s\right)\nabla u_s + \mu_s(\nabla u_s + u_s^T) \quad (28)$$

In the above equation represents the bulk viscosity, which may be obtained as follows;

$$\mu_b = \frac{4}{3}(1-\phi)\rho_s d_p g_o \quad (29)$$

The equation of the solid shear viscosity,μ_s,is derived from [23] as follows;

$$\mu_s = \frac{4}{5}(1-\phi)\rho_s d_p g_o(1+e)\sqrt{\frac{\Theta_s}{\pi}} + \frac{10\rho_s d_p\sqrt{\pi\Theta_s}}{96(1+e)\epsilon g_o}\left[1 + \frac{4}{5}g_o(1-\phi)(1+e)\right]^2 \quad (30)$$

The solid pressure P_s is as following;

$$P_s = (1-\phi)\rho_s\Theta_s + 2(1+e)(1-\phi)^2 g_o\rho_s\Theta_s \quad (31)$$

where Θ_s is granular temperature; e is the coefficient of restitution for particle collisions; g_o is the radial distribution function. For the restitution coefficient, the different values were presented, from 0.18 to 0.4. In the present work, a restitution coefficient value of 0.2 was used from [24]. For the radial distribution function of solid phase, g_o is expressed as [25];

$$g_o = \frac{3}{5}\left[1 - \left(\frac{(1-\phi)}{(1-\phi)_{max}}\right)^{\frac{1}{3}}\right]^{-1} \quad (32)$$

The granular temperature $\Theta_s$is a pseudo-temperature, which can be defined as:

$$\frac{3}{2}\Theta_s = \frac{1}{2}\langle u_s' u_s'\rangle \quad (33)$$

The u_s' is the fluctuating velocity of the particles and can be determined by turbulence kinetic energy as follows:

$$u_s' = \zeta\left(2k/3\right)^{0.5};$$

whereζ is a random number that obeys the Gauss distribution, $0 \leq \zeta \leq 1$.

3. Energy Equation

Gas Phase:

$$\frac{\partial((1-\phi)\rho_s c_{ps} T_s)}{\partial t} + \nabla(\phi\rho_g u_g c_{pg} T_g) = \nabla(\lambda_g.\nabla T_g) + A_s h_s(T_g - T_s) + S_{T_g} \quad (34)$$

Solid Phase

$$\frac{\partial((1-\phi)\rho_s c_{ps} T_s)}{\partial t} + \nabla\left((1-\phi)\rho_s u_s c_{ps} T_s\right) = \nabla(k_{eff}.\nabla T_s) + (\nabla q_r) - A_s h_s'(T_g - T_s) + S_{T_s} \quad (35)$$

The radiative flux density is given by Rosseland (1936) [26] as follows;

$$\nabla q_r = -\frac{16\sigma T^2}{K}(\nabla T)^2 + \frac{16\sigma T^3}{3K}(\nabla^2 T) \quad (36)$$

The thermal dispersion coefficientλ_g can be expressed as:

$$\lambda_g = k_{eff,0} + 0.5 \times d_p \times U_g \times \rho_g \times C_{pg} \quad (37)$$

$$k_{eff,0} = \phi(k_f + h_{rv}\Delta l) + \frac{(1-\phi)\Delta l}{1/(\frac{k_f}{l_v} + h_{rs}) + l_s/k_s} \quad (38)$$

where$l_s = \frac{2d_p}{3}$, $k_s$is the thermal conductivity of the pure solid,l_v,h_{rv}, h_{rs}, and $\Delta l$are written as follows:

$$l_v = 0.151912\Delta l\left(\frac{k_f}{k_{air}}\right) \quad (39)$$

$$h_{rv} = 0.1952\left(1 + \frac{\phi(1-\epsilon)}{2(1-\phi)\epsilon}\right)^{-1}\left(\frac{T_s}{100}\right)^n \quad (40)$$

$$h_{rs} = 0.1952 \times d_p\left(\frac{\epsilon}{2-\epsilon}\right)\left(\frac{T_s}{100}\right)^n \quad (41)$$

$$\Delta l = 0.96795\, d_p(1-\phi)^{-1/3}$$

k_{air} is the air thermal conductivity,

$$k_{air}(T_g) = 5.66 \times 10^{-5} T_g + 1.1 \times 10^{-2} \quad (42)$$

(n) is an empirical parameter related to the fuel packing conditions. In this model,

$$n = 1.93 + 0.67 \exp\left(-\frac{(m_g - 0.39)}{0.054}\right) \quad (43)$$

Source term of the energy equation for both gas and solid is calculated as follows:

$$S_{Tg} = -R_{evp} \times h_{f,CO} \quad (44)$$

$$S_{Ts} = -R_{evp} \times \frac{M_{CO}}{M_{CO_2}} \times \left[h_{f,CO2} - h_{f,CO}\right] \times \left[\frac{Y_{CO}}{2} - 1\right] \quad (45)$$

4. Species Equation

Gas Phase:

$$\frac{\partial(\phi \rho_g Y_{ig})}{\partial t} + \nabla(\phi \rho_g u_g Y_{ig}) = \nabla\left(D_{ig} \nabla(\phi \rho_g Y_{ig})\right) + S_{Y_g} \quad (46)$$

Solid Phase:

$$\frac{\partial((1-\phi)\rho_s Y_{is})}{\partial t} + \nabla((1-\phi)\rho_s u_s Y_{is}) = S_{Y_s} \quad (47)$$

IV. Numerical Method and Boundary Conditions

The transport equations described earlier form a set of nonlinear parabolic partial differential equations can be solved numerically, by using the SIMPLE algorithm. Transport equations are generalized into a standard form;

$$a_{i,j}\Phi_{i,j} + a_{i-1,j}\Phi_{i-1,j} + a_{i+1,j}\Phi_{i+1,j} + a_{i,j-1}\Phi_{i,j-1} + a_{i,j+1}\Phi_{i,j+1} = S_{i,j} \quad (48)$$

The whole geometrical domain of the bed is divided into a number of small cells and (48) is discretized over each cell and solved numerically using SIMPLE algorithm [27], [28].

The feedstock used for the present model was wood pellets. The fuel has a composition (ultimate analysis) of C, 50.4%; H, 6.2%; O, 42.8%. Other properties were ash, 0.4%; total moisture, 8.22%; fixed C, 15.7%; volatiles, 83.9%; LHV, 17.1MJ/kg.

The geometry of the gasifier is approximately symmetrical in the width direction; therefore, the longitudinal section of the gasifier can be used as a 2D geometry. The fuel gas was assumed to leave from the gasifier top. The total number of mesh cells is 100,000. The time step is 10^{-2} s and the gasification time of the biomass were resolved by 480000 time steps. The computational grid was adapted in each time step to the height of the gasifier. The staggered grid was utilized, which set vectors at the boundaries of cells and scalars at the center. The partial differential equations were discretized by the finite volume method (FVM) using the Upwind Difference Scheme.

Table I present operation conditions of 5 selected gasification runs of wood pellets (sized 12mm in diameter). The mass of charge was constant and equal to 20 kg. The temperature of the feed gas varied from 350 up to 900 °C whereas its flow rate was slightly varied from 50 to 56 Nm^3/h. Molar fraction of the steam of the feed gas was varied from 0% up to 83%. All cases the gasification process starts as soon as the feedstock is charged into the gasifier.

TABLE I
Operation Conditions for Run Cases

Case number (-)	Temperature of feed gas (°C)	Total flow of feed gas(Nm^3/h)	Molar fraction of steam in feed gas (%)
C_1	350	50	0
C_2	700	50	0
C_3	830	53	25
C_4	900	53	52
C_5	900	56	83

V. Results and Discussion

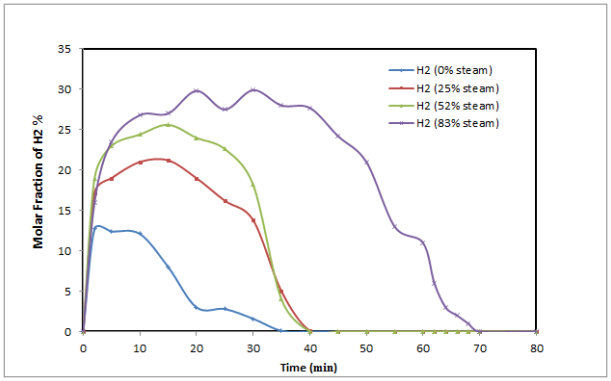

Fig. 2 Changes of the molar fraction of H_2 of the fuel gas for various gasification processes (cases in Table I) gasification of 20kg of wood pellets 12mm

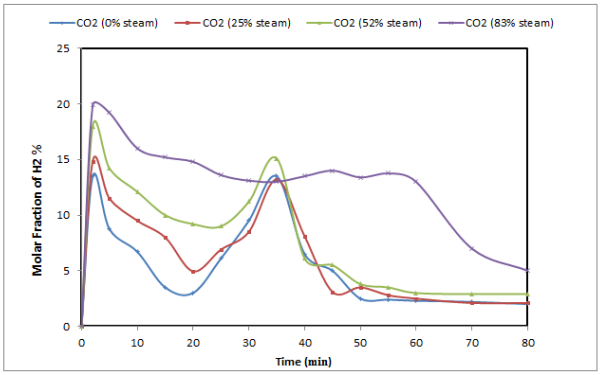

Fig. 3 Changes of the molar fraction of CO_2 of the fuel gas for various gasification processes (cases in Table I) gasification of 20kg of wood pellets 12mm

Figs. 2, 3 show that the higher the molar fractions of steam in the feed gas, the higher the content of hydrogen in the produced gas. Comparing the effect of the feed gas (air and steam) it could be seen that increase of the lower heating value was due to the increases in the molar fraction of the combustible gases (H_2, and CO_2) caused by the pyrolysis process and cracking of hydrocarbons when high-temperature

gasification is applied. The results show that the gasification temperature response to the change of the feed gas composition and temperature of the feed gas.

Results of Computational model and experiments conducted in a high-temperature air/steam fixed bed updraft gasifier presented in Figs. 4, 5 show the capability of this technology of maximizing the gaseous product yield as a result of the high heating rates involved and the efficient tar reduction. Increase of the feed gas temperature reduces production of tars, soot and char residue as well as increases the heating value of the dry fuel gas produced.

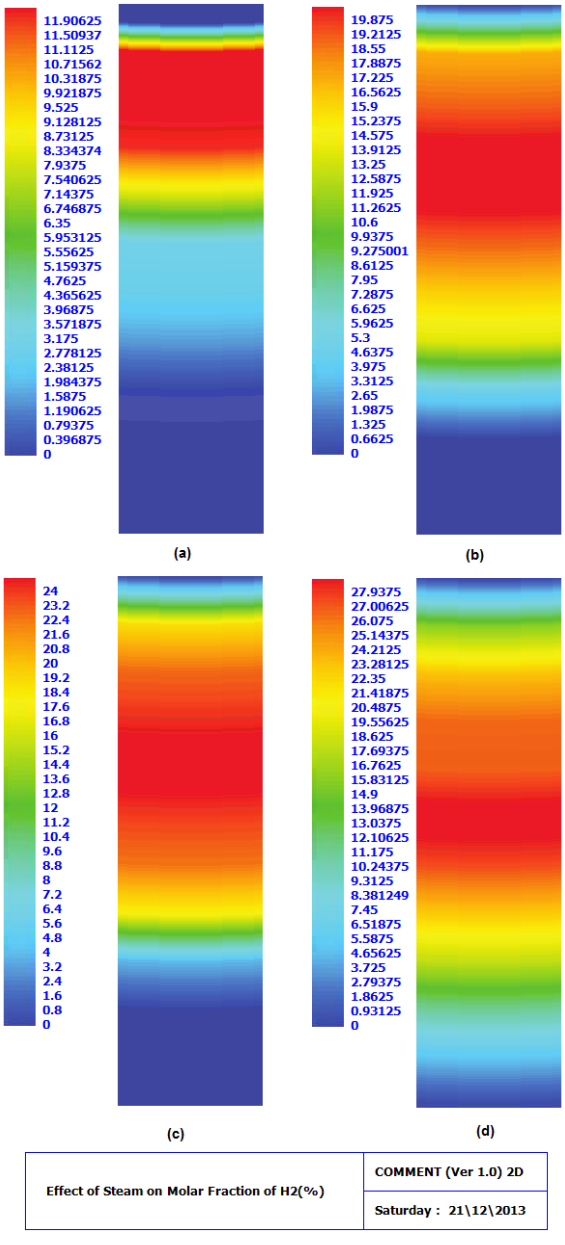

Fig. 4 Effect of steam on molar fraction of H_2 (%) for various gasification processes (cases in Table I) gasification of 20 kg of wood pellets 12 mm); (a) H_2 0%steam, (b) $H_2$25%steam, (c) $H_2$52%steam, (d) $H_2$83%steam

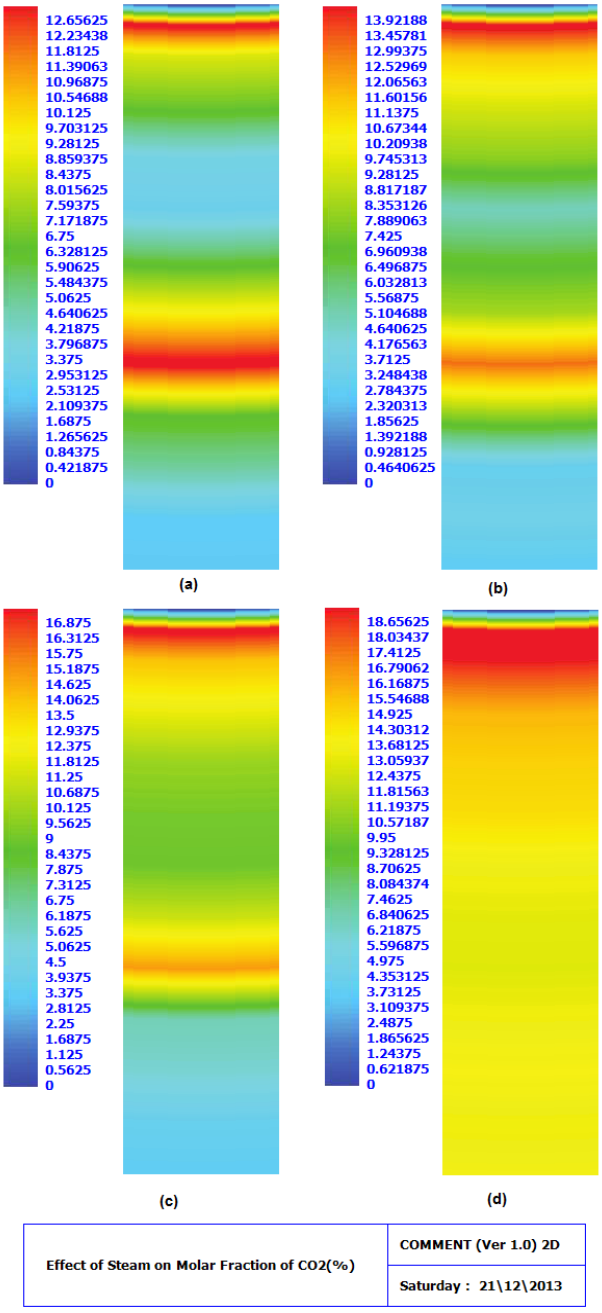

Fig. 5 Effect of steam on molar fraction of CO_2(%)for various gasification processes (cases in Table I) gasification of 20kg of wood pellets 12mm; (a)CO_2 0%steam, (b)$CO_2$25%steam, (c)$CO_2$52% steam, (d)$CO_2$83%steam

A validation for the present model by the experimental set up is used in this study in order to allow a direct comparison with experimental measurements, to validate the presented model to be applicable with different cases for the gasification process in this experiment, the biomass types used for the investigation were Black pellets and Gray pellets. Black pellets are based on the 75% softwood and 25% hardwood, pretreated with a steam explosion. Gray pellets are normal

pellets without pretreatment. Fuel properties and characteristics are given in [16]. The prediction of the composition of the producer gas was in good agreement as shown in Fig. 6, probably caused by the complicated description of pyrolysis model inserted in the present model and also for the sufficient data for the pyrolysis of biomass obtained from experimental works by KTH [29].

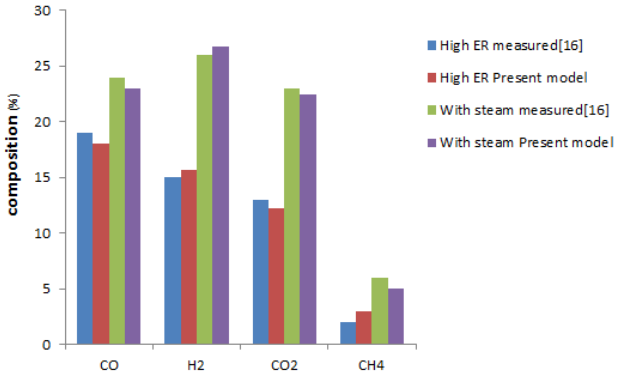

Fig.6 Simulated and experimental effect of steam on syngases composition

VI. Conclusion

A Eulerian-Eulerian CFD model incorporating the kinetic theory of granular flow was applied, by developing a novel mathematical model in the form of COMMENT code applicable for predicting combustion and gasification processes of biomass fuel using high air/steam temperature, giving a promise way in its capability and sensitivity for the parameter effects that influence the gasification process.

Acknowledgment

Many thanks to Associate Professor Weihong Yang at Royal Institute of Technology (KTH) for his continuous support, supervision and the fruitful discussion. Special thanks are directed towards Yueshi Wu for technical supervision in this work during the experimental and theoretical work. We also would like to express our gratitude to all the collaborators from the Royal Institute of Technology.

Nomenclature

A	pre-exponent factor, particle surface area 1/s, m²
C_p	specific heat capacity J/kg K
C_{mix}	mixing rate constant
$C_{w,g}$	moisture concentration in the gas phase kg/m³
$C_{w,s}$	moisture concentration at the solid phase kg/m³
D_g	mass diffusion coefficient of gas m²/s
D_{O2}	mass diffusion coefficient of oxygen m²/s
d_p	particle diameter m
E	activation energy kJ/mol
H_{evp}	evaporation heat of the solid material J/kg
h_f	enthalpy of formation J/kg
h_rs	radiation heat transfer coefficient m/s
h_rv	effective radiation heat transfer coefficient of the voids m/s
h_s	convective mass transfer coefficient
$h_{s'}$	convection heat transfer coefficient W/m² K
I	radiative intensity W
K	extinction coefficient
K	turbulent kinetic energy m²/s²
k_d	diffusion rates kg/atm m² s
k_f	thermal conductivity of the fluid W/mK
k_s	thermal conductivity of the pure W/mK
k_p	absorption coefficient
k_{eff}	effective thermal conductivity W/mK
$k_{eff,0}$	thermal conductivity for no fluid flow W/mK
l_s	equivalent thickness a layer of solid m
M	molecular weight kg/kmol
Q_{cr}	heat absorbed by the solid W
q_r	radiative flux density W
R	gas universal constant J/kmol K
R_{evp}	moisture evaporation rate kg/s
R_c	char consumption rate kg/s
R_{sr}	steam reform reaction kg/s
Rv	volatile matter in solid rate kg/s
R_{wg}	water gas shift reaction kg/s
S_Φ	Source term
T_{env}	environment temperature K
T_g	gas temperature K
T_s	solid temperature K
X	species generation
Y_v	mass fraction of volatile matter
U	velocity component m/s

Greek Letters

A	absorption coefficient
B	drag coefficient
M	dynamic viscosity kg/m s
Φ	void fraction in bed
ε	dissipation rate of turbulent kinetic energy $m^{-2}s^{-3}$
ϵ	Emissivity
σ_p	scattering coefficient
Σ	Stephane-Boltzmann constant W/m² K^4
P	density kg/m³
λ_g	thermal dispersion coefficient
λ_{mix}	effective dispersion coefficient
Φ	dependent variable
τ_s	stress tensor Pa

Subscripts

b	Bulk
C	char burnout
eff	Effective
f	Fluid
g	Gas
p	Particle
s	Solid
sg	solid to gas

References

[1] Y. Wu, Q. Zhang, W. Yang, W. Blasiak, Two-dimensional computational fluid dynamics simulation of biomass gasification in a downdraft fixed-bed gasifier with highly preheated air and steam, Energy &Fuels, 2013, 27, 3274−3282.
[2] W. Jangsawang, A.K. Gupta, K. Kitagawa, S.C. Lee, High temperature steam and air gasification of non woody biomass waste, As. J. Energy Env. , 2007, 8, 601-609
[3] G. Schuster, G. Löffler, K. Weigl, H. Hofbauer, Biomass steam gasification an extensive parametric modeling study, Bioresource Technology, 2001, 77, 71-79.

[4] X. Wang, B. Jin and W. Zhong, "Three-dimensional simulation of fluidized bed coal gasification, Chemical Engineering and Processing: Process Intensification, 2009, 48, 2, 695-705.
[5] M.J.V. Goldschmidt, R. Beetstra, J.A.M. Kuipers, Hydrodynamic modeling of dense gas-fluidized beds: comparison of the kinetic theory of granular flow with 3d hard-sphere discrete particle simulations, Chemical Engineering Science, 2002, 57, 2059–2075.
[6] S. Benyahia, H. Arastoopour, T.M. Knowlton, H. Massah, Simulation of particles and gas flow behavior in the riser section of a circulating fluidized bed using the kinetic theory approach for the particulate phase, Powder Technology, 2000, 112, 24–33.
[7] W. Zhong, Y. Xiong, Z. Yuan, M. Zhang, DEM simulation of gas–solid flow behaviors in spout-fluid bed, Chemical Engineering Science, 2006, 61, 1571–1584.
[8] M.J.V. Goldschmidt, R. Beetstra, J.A.M. Kuipers, Hydrodynamic modeling of dense gas-fluidized beds: comparison and validation of 3d discrete particle and continuum models, Powder Technology, 2004, 142, 23–47.
[9] J. Ding, D. Gidaspow, A bubbling fluidization model using kinetic theory of granular flow, AIChE Journal, 1990, 36, 523–538.
[10] D. Gidaspow, multiphase flowand fluidization: continuum and kinetic theory description, Academic Press, San Diego, 1994.
[11] V. Mathiesen, T. Solberg, B. H. Hjertager, An experimental and computational study of multiphase flow behavior in a circulating fluidized bed, international journal of multiphase flow, 2000, 26, 387–419.
[12] W. Zhong, M. Zhang, B. Jin, Z. Yuan, Flow behaviors of a large spout-fluid bed at high pressure and temperature by 3dsimulation with kinetic theory of granular flow, Powder Technology, 2007, 175, 90–103.
[13] L. Yu, J. Lu, X. Zhang, S. Zhang, Numerical simulation of the bubbling fluidized bed coal gasification by the kinetic theory of granular flow (KTGF), Fuel, 2007, 86, 722–734.
[14] T.M. Ismail, M. Abd El-Salam, M.A. El-Kady, S.M. El-Haggar, three dimensional model of transport and chemical late phenomena a MSW incinerator, International Journal of Thermal Sciences, 2014, 77, 139-157.
[15] W. Yang, A. Ponzio, C. Lucas, W. Blasiak , Performance analysis of a fixed-bed biomass gasifier using high-temperature air, Fuel Processing Technology, 2006, 87, 235 – 245.
[16] D. S. Gunarathne, J. K. Chmielewski, W. Yang, high temperature air/steam gasification of steam exploded biomass, International Flame Research Foundation. The Finnish and Swedish National Committees Finnish – Swedish Flame Days, 2013
[17] C. Lucas, D. Szewczyk, W. Blasiak, S. Mochida, High-temperature air and steam gasification of densified biofuels, Biomass and Bioenergy, 2004, 27, 563–575.
[18] B. Peters, N. Thomas, B. Christian. Modeling wood combustion under fixed bed conditions, Fuel, 2003, 82, 729–738.
[19] B. Tabrizi, A. Saffar, M. R. Assarie, Two-dimensional mathematical model of a packed bed dryer and experimentation, Journal of Power and Energy, 2001, 216, 161-168.
[20] Di Blasi C. Modeling wood gasification in a countercurrent fixed-bed reactor, AIChE J, 2004, 50, 9.
[21] J. Cooper, W. L. H. Hallett. A numerical model for packed-bed combustion of char particles. Chemical Engineering Science, 2000, 55, 4451–4460.
[22] Launder, b. E. and Spalding, D. B. The numerical computations of turbulent flows.1974.
[23] D. Gidaspow, A bubbling fluidization model using kinetic theory of granular flow. AIChE Journal, 1994, 32, 1, 523–538.
[24] S. Hermann, Boundary layer theory. McGraw-Hill, 1979, Seventh Edition.
[25] H. Arastoopour, Numerical simulation and experimental analysis of gas-solid flow systems: 1999 fluor-danielplenarylecture, Powder Technology, 2001, 119, 59-67.
[26] Rosseland, S., Theoretical Astrophysics: Atomic Theory and the Analysis of Stellar Atmospheres and Envelopes, Oxford, UK: Clarendon, 1936.
[27] S.V. Patankar, Numerical heat transfer and fluid flow, Hemisphere, 1980.
[28] W.Q. Tao, Numerical Heat transfer, Second Ed., Xi'an Jiaotong University, Xi'an, 2001.
[29] W. Blasiak, D. Szewczyk, C. Lucas, S. Mochida, Proceedings of 21st International Conferences on Incineration and Thermal Treatment Technologies, May 13–17, 2002, New Orleans, Louisiana, USA, 2002.